



Radioactivity induced in new-generation cardiac implantable electronic devices during high-energy X-ray irradiation

Adam Konefał^{a,*}, Sławomir Blamek^b, Aleksandra Wrońska^c, Andrzej Orlef^d, Maria Sokół^d, Mateusz Tajstra^e, Mariusz Gąsior^e

^a Institute of Physics, University of Silesia in Katowice, Katowice, Poland

^b Maria Skłodowska-Curie National Research Institute of Oncology, Gliwice Branch, Department of Radiotherapy, Gliwice, Poland

^c Marian Smoluchowski Institute of Physics, Jagiellonian University, Kraków, Poland

^d Maria Skłodowska-Curie National Research Institute of Oncology, Gliwice Branch, Department of Medical Physics, Gliwice, Poland

^e 3rd Chair and Department of Cardiology, Silesian Center for Heart Diseases in Zabrze, Medical University of Silesia, Katowice, Poland

ARTICLE INFO

Keywords:

CIEDs
Induced radioisotopes
Nuclear reactions
Radiotherapy

ABSTRACT

This study provides the first insight into the problem of the induced radioactivity of the construction materials of the new-generation cardiac implantable electronic devices (CIEDs). Its aim was to identify nuclear reactions and the resulting radioisotopes induced in the CIEDs by high-energy X-ray therapeutic beams generated by medical linear accelerators. The presented results allow to verify the rightness of choice of materials for investigated CIEDs. Such analysis is currently available only for the older types of the CIEDs, but not for those of the new generation. Gamma spectrometry measurements have been performed using a high-purity germanium detector (HPGe). The identification and activities of the generated radioisotopes were obtained from the measured spectra of gamma - rays from decays of the produced unstable radioisotopes. 21 radioisotopes originating from 24 nuclear reactions were identified. For all considered models of CIEDs the highest activities are from the tin isomer ^{117m}Sn . The induced activities were relatively small, not exceeding 3.1 Bq per a 1 Gy X-ray dose to a target volume.

1. Introduction

Cardiac implantable electronic devices (CIEDs) are usually placed in a subcutaneous pocket over the pectoral muscles in the infraclavicular region. This location poses a problem for dose delivery in radiotherapy of breast, lung, head and neck, lymphomas, thyroid and oesophageal cancers. According to literature and our previous results (Blamek et al., 2016), the CIEDs are prone to various radiation damages during the exposure to X-ray therapeutic beams. The main factor causing such damages are contamination neutrons produced both in X-ray therapy as well as in proton therapy, performed with the use of medical accelerators of various types (Ma et al., 2002; Konefał et al., 2005, 2008a; Biltekin et al., 2015). The secondary neutrons in X-ray therapy result from (γ, n) reactions with high atomic number materials in the massive components of accelerators (Mao et al., 1997), mainly in the head of a linac. The neutrons move around essentially isotropically (Kry et al., 2005). Neutron contamination is a serious area of interest in terms of induction of nuclear reactions and secondary cancers. In accelerators

generating high-energy photons and protons, neutrons originate from photonuclear reactions (γ, n) , $(\gamma, 2n)$, $(\gamma, 3n)$ and proton-induced nuclear reactions (p, n) , $(p, p' n)$. The energy threshold of these reactions is about 8 MeV for most isotopes (Dietrich and Bermab, 1998; Ditróí et al., 2016). The cross sections for the photonuclear reactions have a resonant character with a maximum depending on the atomic number. The produced neutrons are characterized by a broad energy range (Vega-Carrillo and Baltazar-Raigosa, 2011; Howell et al., 2009; Esposito et al., 2008; Vega-Carrillo et al., 2012; Santa, 2017; Talebi et al., 2016).

There are many works describing the malfunctions of cardiac implantable electronic devices after high-energy radiation exposure. In microprocessors based on small voltage surges, a single neutron passing through random access memory (RAM) may leave voltage ripples or wakes, which lead to the reprogramming of the software code or bits, from 1 to 0 and *vice versa* (Baumann, 2001). As a result, some functions of an electronic device may work incorrectly. This phenomenon is usually called single event effects (SEE). Such single ionization events may lead to a temporary or permanent damage of electronic devices or

* Corresponding author.

E-mail address: akonefal@us.edu.pl (A. Konefał).

<https://doi.org/10.1016/j.apradiso.2020.109206>

Received 18 January 2020; Received in revised form 27 March 2020; Accepted 24 April 2020

Available online 1 May 2020

0969-8043/© 2020 Elsevier Ltd. All rights reserved.

systems. It is an important effect for digital circuits such as memories or microprocessors. SEEs induced by neutrons in microelectronic devices were studied and confirmed (Bisello et al., 2012). These effects can be caused even by single neutrons, like atmospheric neutrons at sea level (Leray, 2007), despite their very small fluence, of about 10 neutrons/hour/cm² (Leray, 2007), or by other natural sources of radiation (O'Gorman et al., 1996; Wang et al., 2007). Neutron-induced single event upsets were also observed in neurostimulators of similar construction like cardiac devices (Dong et al., 2016).

The neutrons produced in accelerators can cause nuclear reactions in all objects in the neutron field. In the case of medical accelerators the neutron-induced reactions occur in collimators of beams, radiation shields, targets, accelerator accessories, walls of accelerator facility etc. (Polaczek-Grelak et al., 2012; Konefal et al., 2008b). As a result, various radioisotopes appear and the accelerator components become radioactive (Vega-Carrillo et al., 2015; Janiszewska et al., 2014; Konefal et al., 2016; Bieniasiewicz et al., 2016) and are a source of additional dose to the operating staff (Hashemi et al., 2007; Barquero et al., 2002; Alem-Bezoubiri et al., 2014; Keehan et al., 2016; Choi et al., 2018; Elham et al., 2018). Any damages of the CIEDs due to radiation may cause their malfunctioning and, consequently, a serious danger to the patient's life.

The aim of this work was the identification of the nuclear reactions and the radioisotopes induced in the CIEDs by high-energy X-ray therapeutic beams generated by medical linear accelerators applied in telerradiotherapy. Most oncology centers use 6 MV X-ray therapeutic beams for patients with implanted cardiac devices to avoid neutron irradiation of CIEDs as well as to reduce a scattered photon dose to them. Thus, the radioisotopes are rarely activated in CIEDs during radiotherapy. However, as the linear accelerators can often delivered also high-energetic photon beams (>6 MV), specific tumours of patients with CIEDs might be treated with higher-energy X-rays (from 15 MV to 23 MV) (Gauter-Fleckenstein et al., 2015). In order to eliminate the potential risk of CIED activation the manufacturers should avoid using certain isotopes when manufacturing those devices.

Three modern CIED models, being currently on the market, but not tested in this respect yet, were compared. These CIEDs are used as implantable cardioverter defibrillators (ICDs) and cardiac resynchronization therapy devices with a function of defibrillators (CRT-D). Their systems differ significantly from the older models (Bitterman et al., 2018), whereas in the professional literature the radiation investigations only for the older types of the CIEDs (Zecchin et al., 2018; Mollerus et al., 2014; Blamek et al., 2014) have been described. Modern CIEDs contain Complementary Metal Oxide Semiconductor (CMOS) technology. In a radiation environment CMOS device may be subjected to a continuous dose of particle radiation that causes degradation of performance, increase in leakage current, and ultimately failure of the device (Bisello et al., 2012). The older versions of CIEDs operated at lower power supply voltage and therefore they were more sensitive to electric charge produced and accumulated in them. However, since the early nineties CMOS technology has rapidly developed and currently is much more radioresistant (Hurkmans et al., 2012). Nevertheless, modern CIEDs are equipped with extra electronic modules providing additional functionalities – they can work as implantable cardioverter defibrillators (ICDs) and cardiac resynchronization therapy devices with a function of defibrillators (CRT-D). Thus, because of the increasing complexity, their sensitivity to radiation increases.

The latest recommendations of the Heart Rhythm Society (HRS) (Indik et al., 2017) delineate practical solutions for health care providers of various backgrounds for the management of patients with CIEDs undergoing radiation exposure so they can be imaged and treated in a manner that balances benefit and risk, while recognizing that risk cannot be eliminated. They are based on the results gathered within 2003–2014 (Brambatti et al., 2015; Zaremba et al., 2015) for the older types of the CIEDs, some of them currently not in use.

In order to identify the radioisotopes and the nuclear reactions

induced in the CIEDs exposed to ionization radiation, gamma-ray spectroscopy was applied.

2. Methods

The different models of CIEDs by three manufacturers (Lumax 340 DR by Biotronik, Maximo II DR by Medtronic, 3213–36 Promote RF by St Jude) presented in Fig. 1 were activated in the therapeutic X-ray beams of 10 MV and 20 MV generated by the TrueBeam linear accelerator by Varian (Fig. 2) used in telerradiotherapy in the Center of Oncology in Gliwice (Poland). The radioisotopes induced in the CIEDs were identified spectroscopically from the spectra of gamma-rays from the radioactive decays. In the case of 10 MV and 20 MV X-ray beams the photon field is contaminated by neutrons originated from photonuclear reactions. The CIEDs were located in the therapeutic beam and activated in the mixed photon-neutron field. The effects from therapeutic photons and neutrons are distinguishable: the photon-activation results from the photonuclear reactions and occurs only in the therapeutic beam, whereas the neutron activation takes place also outside the beam. The neutron fluence is approximately constant in the treatment room and on the surface of a patient body (Kry et al., 2005). Thus, the results obtained in the neutron reactions are expected to be the same for any location of the CIEDs inside and outside the therapeutic beam. We decided to locate the CIEDs in the beam to broaden the scope of possible clinical situations and include a case when a body region with a CIED is directly exposed to radiation. It is not such a rare situation, because according to the Recommendations and Protocol for the Management of the CIED Patient Undergoing Radiation Therapy (Indik et al., 2017) and the European Heart Rhythm Association survey (Lenarczyk et al., 2017) a surgical relocation of the device and a continuous CIED relocation in the cardio-oncologic patients is optional and suggested only if it will interfere with an adequate tumor treatment. The main recommendations involve also a complete CIED evaluation performed before and during radiotherapy, choosing, if possible, a non-neutron-producing treatment to minimize the risk of device reset, and performing of weekly complete CIED evaluations for the patients undergoing neutron-producing treatment. Moreover, CIED relocation is not recommended for the devices receiving a maximum cumulative incident dose of <5 Gy, or when tumor disease makes it impossible to relocate a CIED.

2.1. Identification of radioisotopes induced in activated CIEDs

Spectroscopic identification of the radioisotopes induced in the CIEDs by radiation exposure was done with three ORTEC detection systems composed of a high-purity germanium detector (Fig. 3a) cooled with the use of liquid nitrogen, connected to a multichannel analyzer read out via the Tukan8k software. Such high resolution detectors (HPGe) are suitable for investigation of samples containing many radionuclides (e.g. from the natural radioactive series), when the gamma-ray spectrum presents a large number of peaks to be resolved.

The spectra were acquired in the range of energies from 100 keV to 2.3 MeV. A set of commercial calibration sources (⁶⁰Co, ¹³⁷Cs, ¹⁵²Eu) was applied for the energy calibration of the detectors. For all of them

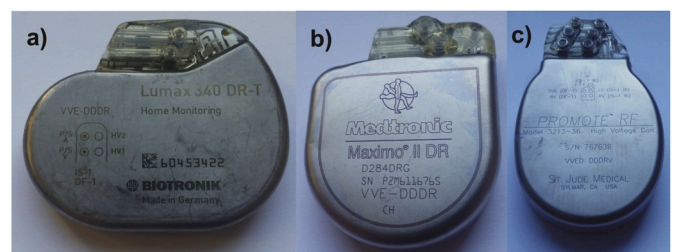


Fig. 1. Lumax 340 DR by Biotronik (a), maximo II DR by medtronic (b), 3213–36 promote RF by St Jude (c).



Fig. 2. The TrueBeam linear accelerator by Varian used for irradiation of CIEDs.

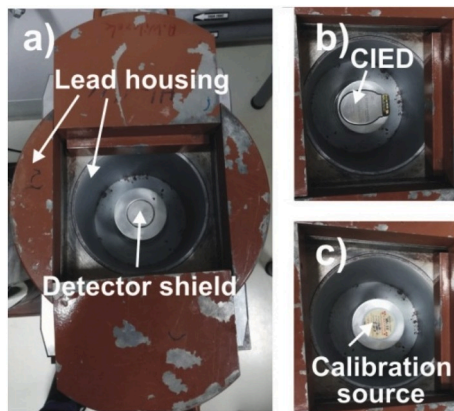


Fig. 3. High-purity germanium detector (HPGe) inside a lead housing (a). Location of a CIED (b) and a calibration source (c) on the aluminum shield of the HPGe detector during the gamma - ray spectra acquisition and the calibration, respectively.

the determined energy calibration curve was linear. The working parameters of the detectors were chosen in such a way that the difference between the energies corresponding to two neighboring channels was 0.3 keV and the full width at half maximum (FWHM) of the peak at 1332.5 keV from the ^{60}Co decay equaled 1.2 keV. The radioisotope identification method was verified using natural samples including uranium series. For each CIED under study the first measurement was performed directly after activation. The time between the end of the CIED irradiation and the beginning of the spectroscopic measurement did not exceed several minutes. Additionally, the spectra were registered for about two weeks in a continuous manner, which made it possible to determine the half-lives for most of the identified radioisotopes. The measurements were performed in the operating rooms of the accelerators (directly after the activation of CIEDs) as well as in the Department of Nuclear Physics and Its Application in the Institute of Physics of the University of Silesia in Katowice (Poland). The CIEDs were put on the top surface of the HPGe detector shield (Fig. 3b). The spectra were analyzed using the tables of isotopes edited by Firestone (1996) and the

neutron reaction cross sections from the open data bank of the Brookhaven National Laboratory (<http://www.nndc.bnl.gov/s>).

2.2. Quantitative analysis for radioisotopes induced in activated cardiac pacemakers

For the purpose of the quantitative analysis, the efficiency of the detector has to be determined in a required energy range. The detection efficiency ε measures the ability of the detector to convert gamma-rays into useful signals. It can be expressed by the following equation:

$$\varepsilon(E) = 100 \cdot A_{CS} \cdot N_d(E)^{-1} \cdot t_p, \quad (1)$$

where.

A_{CS} – the activity of an isotropic radiation source located on the surface of the detector shield (Fig. 3c),

$N_d(E)$ – events collected in a photopeak (a net area) at energy E in the calibration measurement,

t_p – the time of the calibration measurement.

It is worth to stress, that efficiency defined this way contains already the factor related to the geometrical acceptance. In the efficiency calibration the commercial source of ^{152}Eu was applied, with a linear size of 0.1 mm. The source was sealed in a plastic cylindrical capsule (2 mm high and 5 mm in diameter) and placed on the top surface of the HPGe detector shield, in uniformly distributed locations, as shown in Fig. 4a. The measuring locations covered the surface of the detector shield in the region determined by the shape and the sizes of the CIEDs. The distances between the locations were constant. The mean net area calculated for the spectra acquired in all measuring locations at each considered energy was taken for the determination of the efficiency curve for each used HPGe detector. Such approach makes it possible to reduce the systematic uncertainty related to the differences between the shapes of the investigated CIEDs and the calibration source. The summing effect, which can be seen especially for an efficiency curve at low and intermediate energy region, was corrected using the Monte Carlo simulation (GEANT4 code). The net area of each photopeak was obtained from a Gaussian fit and the background modeled with a polynomial. The detection efficiency as a function of energy E of gamma-rays can be described by the simple power function (Fig. 4b). The activities of the identified radioisotopes were calculated on the basis of the net areas of the most pronounced photopeaks in the spectra corrected for the HPGe detector efficiency. If possible, to separate overlapping photopeaks of two different radioisotopes the differences in their half-lives were employed, otherwise a net area of another photopeak with a smaller intensity was taken into account to estimate activity. The determined activity of a radioisotope, related to the end of the CIED irradiation can be described by the following formula:

$$A = 100 \cdot N_d'(E) \cdot I(E)^{-1} \cdot \varepsilon(E)^{-1} \cdot (1 - e^{-\lambda \cdot t_p})^{-1} \cdot e^{\lambda \cdot t_a}, \quad (2)$$

where,

$N_d'(E)$ – events collected in a photopeak at energy E in the measurement with CIEDs,

$I(E)$ – emission intensity of the gamma-rays forming the photopeak at E,

t_p' – the time of the measurement of energy spectrum of gamma-rays emitted by activated CIED,

t_a' – the time between the end of the CIED activation and the beginning of the spectroscopic measurement,

λ – the decay constant for the identified radioisotope.

formula (2) includes the correction of decrease in the activity occurring during the measurement of the gamma-ray spectrum.

The uncertainties of the net areas did not exceed 1% for most of the

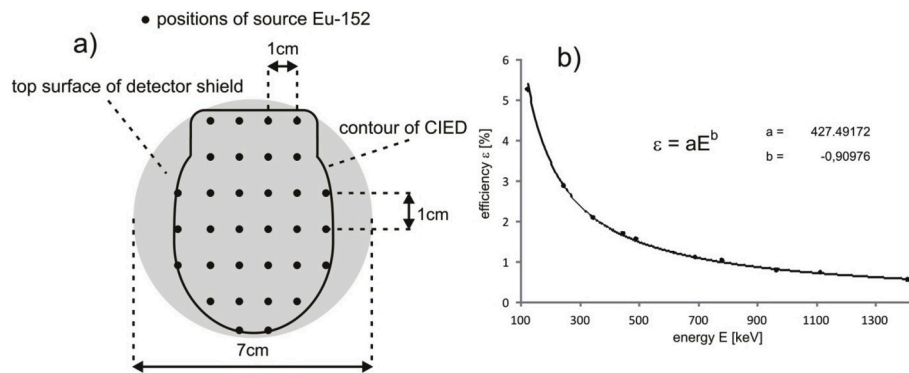


Fig. 4. a) The positions of a ^{152}Eu source on the top surface of the HPGe detector shield in the efficiency calibration measurements. b) The efficiency curve of one of the HPGe detector used in this work.

photopeaks used in the calculations of the radioisotope activities. Gamma-rays scattered and absorbed in the materials of the CIEDs do not contribute to the registered photopeaks and this loss was not taken into account in the quantitative analysis because the CIEDs were not dismantled.

Additionally, a dose rate from gamma-rays was measured by a radiometer for each CIED immediately after activation by the 20 MV X-ray beams. In these measurements the CIED was located on the radiometer window, to estimate the dose rate to tissues adjoining to the device surface.

To ensure statistical sensitivity for the elements, whose content in the investigated devices was very small, a large radiation dose related to 9000 monitor units was emitted. One monitor unit corresponded to the dose of 1 cGy delivered to the target volume. The obtained activities of radioisotopes in the CIEDs were related to the dose of 1 Gy to increase the clinical relevance of results. The details of beam parameters used for irradiation of CIEDs are included in Table 1.

3. Results

3.1. Qualitative analysis of spectra of gamma-rays emitted by the activated CIEDs

The basic activation of the CIEDs was performed in the therapeutic 20 MV X-ray beam from the TrueBeam accelerator. The spectra registered directly after the activation are presented in Figs. 5–7. Due to the high energy of used X-rays and the neutron radiation around the treatment units, there is a number of possible reaction channels and, consequently, a variety of produced radioisotopes contributing to the resulting gamma spectra.

Fig. 8 shows the spectrum acquired from the same model of St Jude CIED as described in Fig. 5, but this time activated in the therapeutic 10 MV X-ray beam. The maximum energy of the photons was only

Table 1

Characteristic of the therapeutic beams and the irradiation conditions used for irradiation of CIEDs.

Parameter	10 MV beam (FFF)	20 MV beam (FF)
^a Average energy [MeV]	2.3	4.5
^a Peak energy [MeV]	0.2	1.9
^a Maximum energy [MeV]	11.0	22.0
Pulse width [μs]	4	4
Irradiation time [min]	15	15
Dose rate [MU/min]	600	600
Radiation field size	$10 \text{ cm}^2 \times 10 \text{ cm}^2$	$10 \text{ cm}^2 \times 10 \text{ cm}^2$
^b SSD [cm]	100 cm	100 cm

^a Determined using the Monte Carlo simulations (GEANT4 code).

^b Source-Surface Distance – here, a distance between the beam source and the CIED surface.

somewhat higher than the energy threshold of the photonuclear reactions for most isotopes.

The detailed analysis of the photopeaks in the measured spectra made it possible to identify the induced radioisotopes and the nuclear reactions (Fig. 9a and b).

Altogether, 21 radioisotopes originating from 24 nuclear reactions were identified for three considered models of the CIEDs (Table 2). Four of them ($^{99\text{m}}\text{Tc}$, $^{177\text{m}}\text{Sn}$, $^{106\text{m}}\text{Ag}$, $^{92\text{m}}\text{Nb}$) are the metastable isomers. 6 radioisotopes were created directly by the photonuclear reactions induced by the high-energy therapeutic X-ray beams. 5 radioisotopes presumably originate from the photonuclear reactions as well as from the neutron-induced ones. Other 8 identified radioisotopes are the products of the neutron-induced reactions, mainly simple capture reactions that are characterized by relatively large cross sections for thermal neutrons and particularly by the high resonances in the energy range of slowed down neutrons. 3 radioisotopes are the result of radioactive decays. We failed to identify the reaction from which the radioisotope ^{48}V originates (the number 19 in Fig. 9b).

The maxima of cross sections for the identified photonuclear reactions are included in Table 3, whereas those for the identified simple capture reactions for thermal neutrons are presented in Table 4, where the highest resonances are also listed. The radioisotopes of ^{57}Ni , ^{57}Co , ^{196}Au and ^{197}Au were observed for all three models irradiated with 20 MV X-rays. The radioisotopes of ^{56}Mn , ^{99}Mo and $^{99\text{m}}\text{Tc}$ appeared only for the CIEDs by St Jude. The radioisotopes - ^{111}Ag , ^{48}V , $^{92\text{m}}\text{Nb}$ were observed only for the device by Medtronic. The radioisotopes of copper ^{64}Cu and ^{66}Cu and scandium ^{46}Sc were identified in the models by Biotronik and Medtronic, whereas the radioisotopes of arsenic ^{74}As and ^{76}As are induced in the models of St Jude and Medtronic. The radioisotopes of chromium ^{51}Cr and manganese ^{54}Mn were observed for the models of St Jude and Biotronik.

In the case of the model by St Jude 15 radioisotopes were identified after the exposure to 20 MV X-ray radiation, whereas only 5 radioisotopes were observed when 10 MV X-rays were used. Eight of them originate from the photonuclear reactions. ^{56}Mn results from the simple capture reaction ($\sigma_{\text{ther}} = 13.2 \text{ b}$) and is characterized by a short half-life (the shortest one is for ^{66}Cu). However, the copper radioisotopes were not observed in this CIED model even when irradiated with 20 MV X-rays. As shown in the study by Konefal et al. (2016) the neutron fluence from 10 MV X-rays is about three orders of magnitude smaller than that from 20 MV X-rays beam for the TrueBeam linac, and this effect is clearly responsible for the observed difference in the corresponding activations.

Identification of the β^+/β^- emitters decaying without the emission of gamma-rays is difficult. Their direct identification is hampered because of the short ranges of electrons and positrons in solids, usually not exceeding a fraction of a millimeter. However, the presence of certain gamma emitters in the CIEDs means that some β^- and β^+ radioisotopes emitting no gamma-rays have to be produced in the reactions with more

St Jude

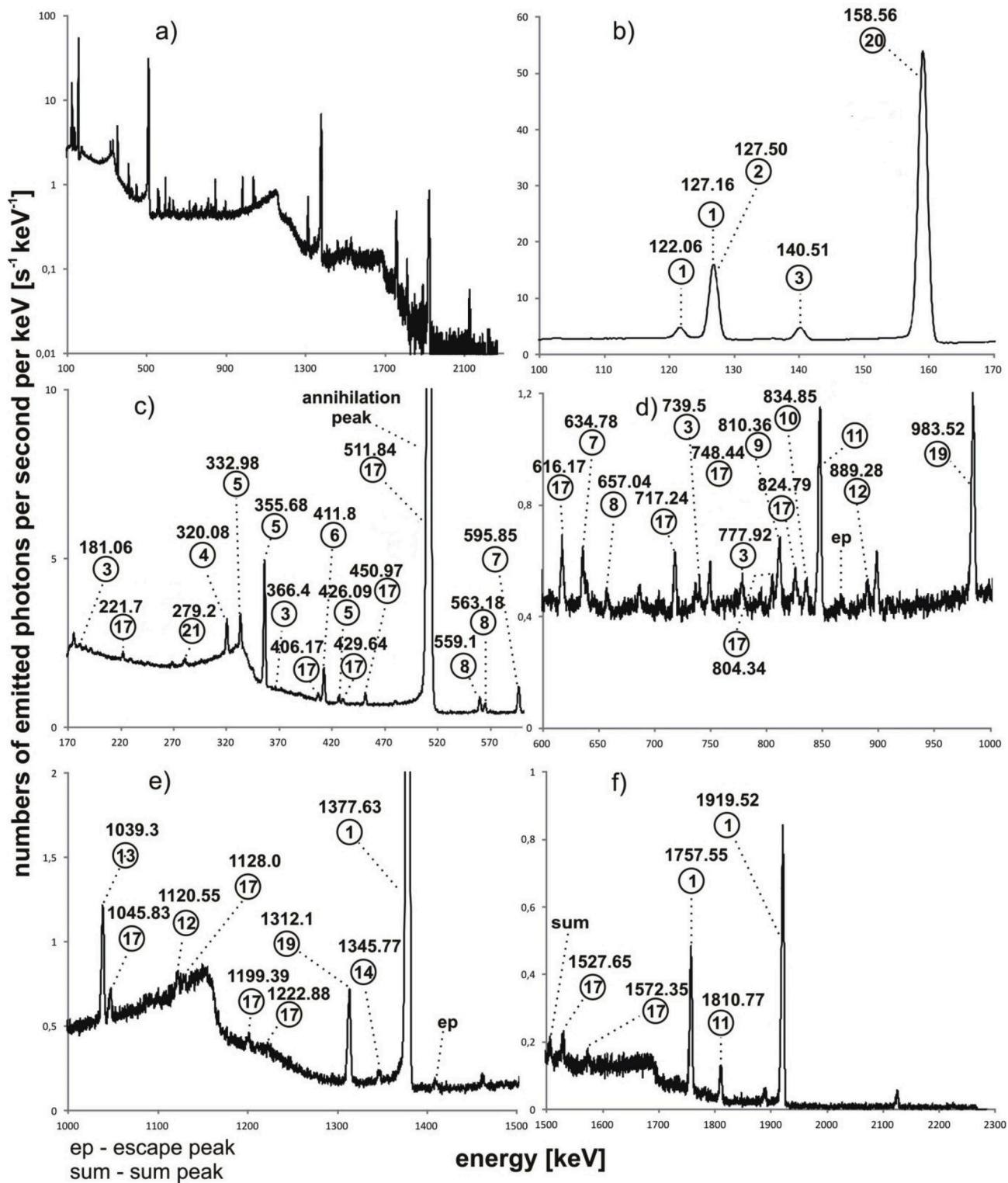


Fig. 5. a) The spectrum of gamma-rays emitted by the activated St Jude CIED after 20 MV beam irradiation in the full energy range (the vertical axis is logarithmic). b) – f) Sub-ranges of the spectrum presented in a) chosen for a detailed presentation. All identified photopeaks are denoted by their energies (in keV) and the numbers related to the nuclear reactions (see Fig. 9).

abundant isotopes. The production of several radioisotopes of ¹²¹Sn, ¹²³Sn and ⁶²Cu can be confirmed this way (details in Table 5).

3.2. Results of the quantitative analysis

The activity of an induced radioisotope depends on the amount of a target isotope, a half-life of the induced radioisotope and a cross section

Biotronik

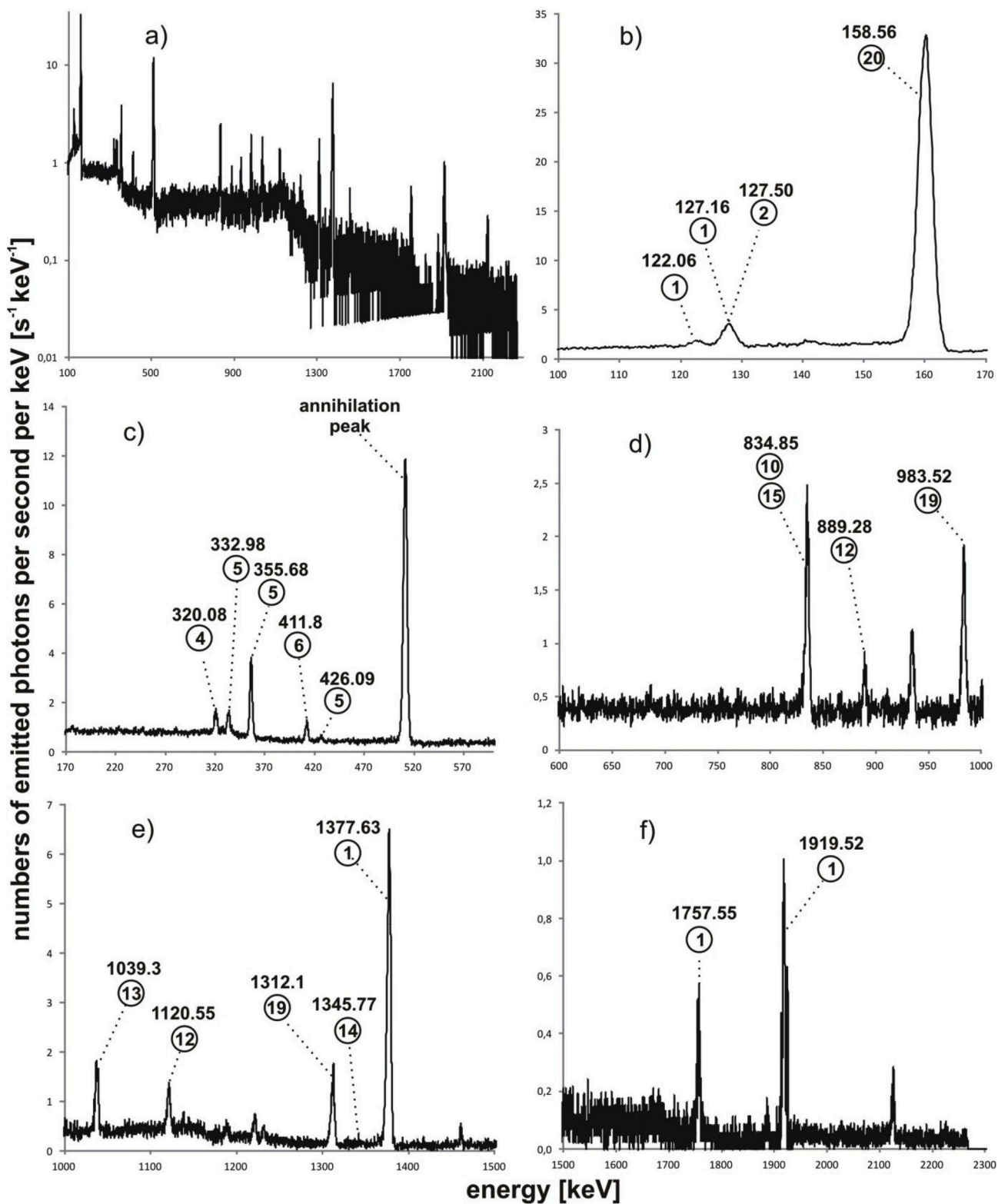


Fig. 6. a) The spectrum of gamma-rays emitted by the activated Biotronik CIED after 20 MV beam irradiation in the full energy range and b) – f) its zoomed sub-ranges. Otherwise as in Fig. 5.

Medtronik

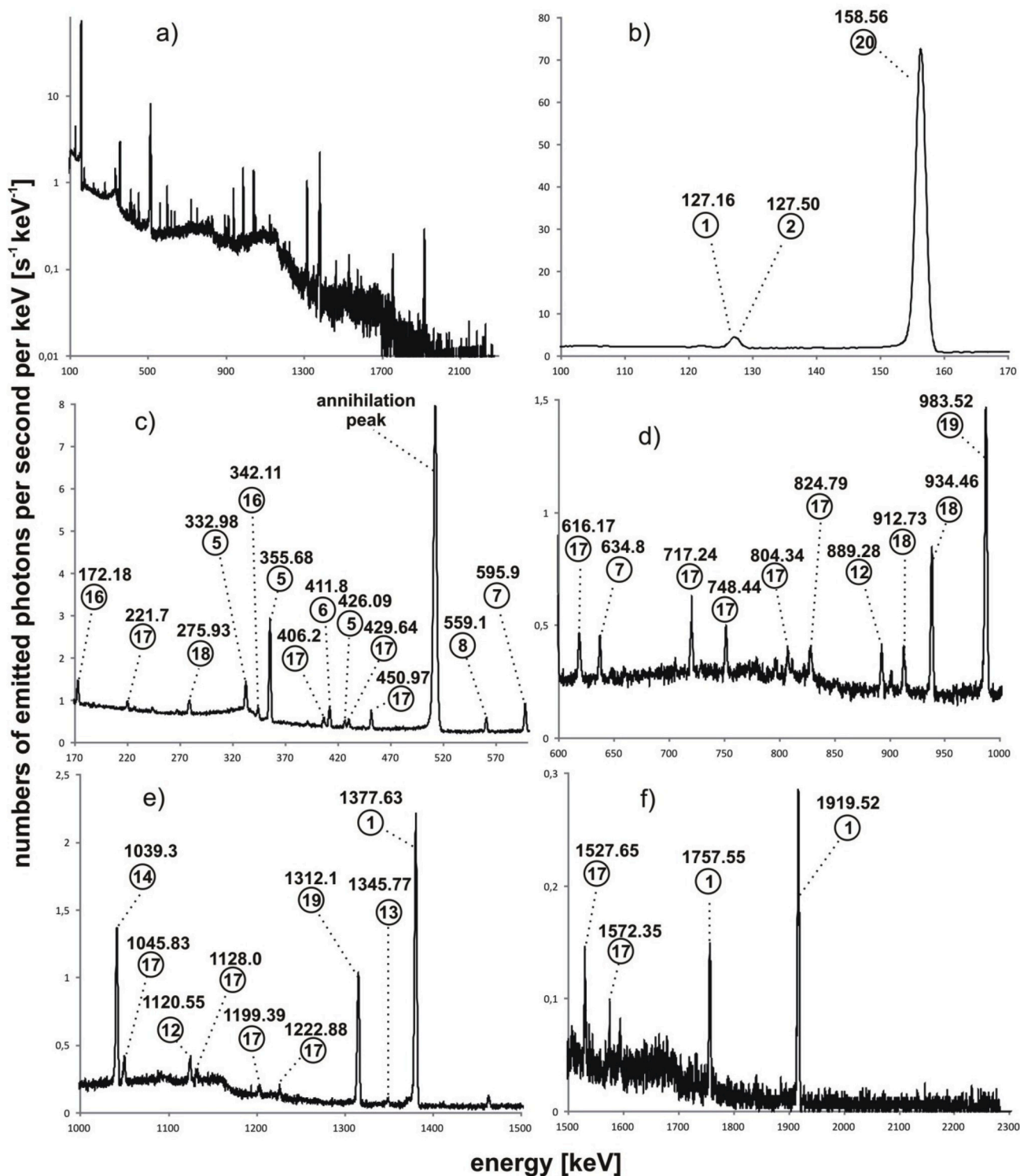


Fig. 7. a) The spectrum of gamma-rays emitted by the activated Medtronik CIED after 20 MV beam irradiation in the full energy range and b) – f) its zoomed sub-ranges. Otherwise as in Fig. 5.

for the nuclear reaction in which the radioisotope is produced. The maximum activities of the radioisotopes induced in the CIEDs during emission of the 20 MV X-ray therapeutic beam are relatively small, not exceeding 1.889 Bq/Gy to the target volume (Table 2) for the identified gamma-ray emitters. For all three models the highest measured activities come from the tin isomer ^{117m}Sn . In the case of the St Jude CIED the

next most abundant radioisotopes are ^{57}Ni and ^{51}Cr , whereas for the Biotronik device the next two are ^{66}Cu and ^{57}Ni and for the CIED by Medtronik, the copper radioisotopes ^{64}Cu and ^{66}Cu . In spite of the largest number of the identified radioisotopes the St Jude CIED has the lowest total activity of all three considered models, being 2.182 Bq/Gy (the sum of the activities of all induced radioisotopes). The devices by

St Jude after 10 MV irradiation

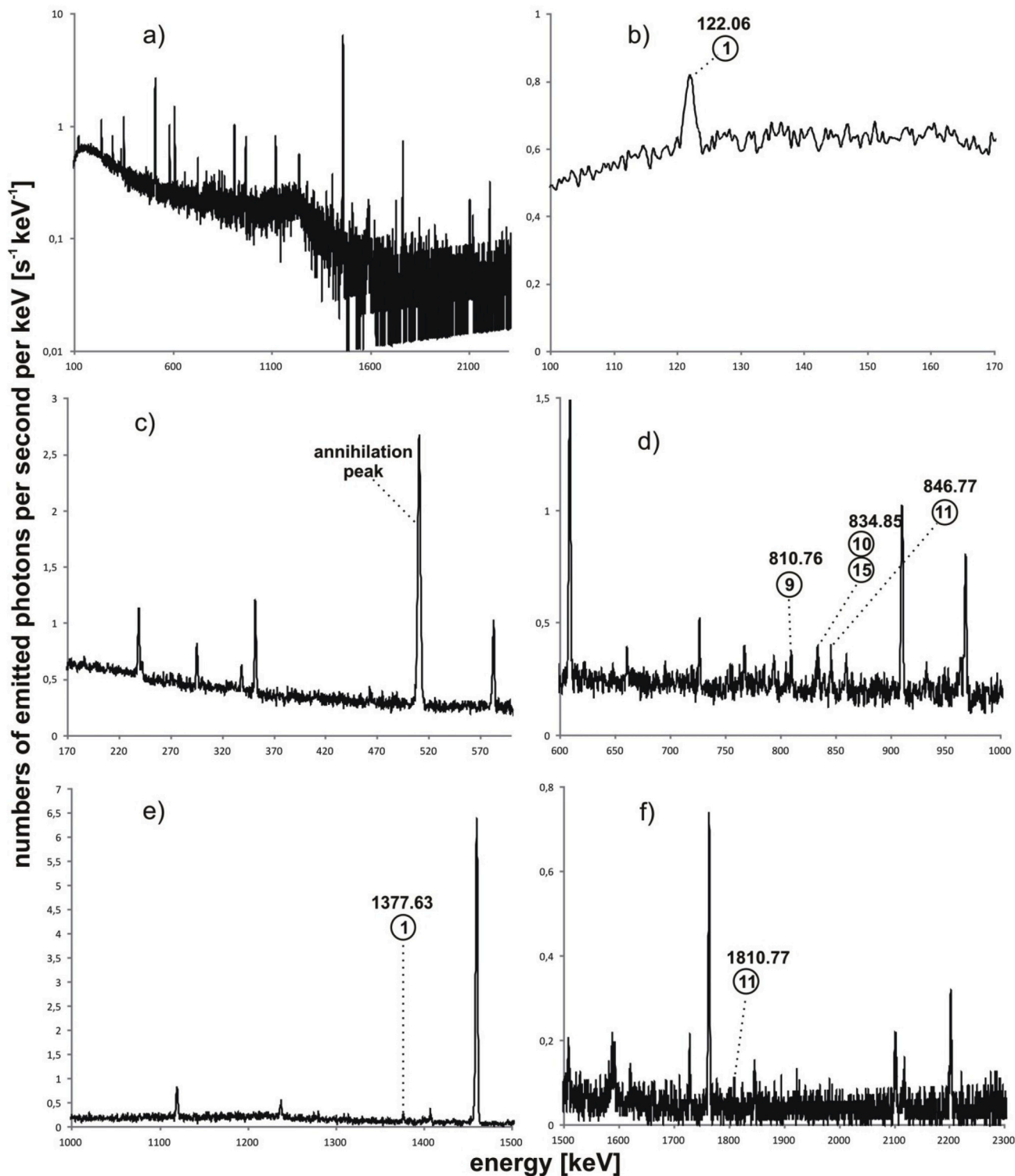


Fig. 8. a) The spectrum of gamma-rays emitted by the activated St Jude CIED model after activation in the therapeutic 10 MV X-ray beam in the full energy range and b) – f) its zoomed sub-ranges. The photopeaks which are not labelled originate from natural radioisotopes. Otherwise as in Fig. 5.

Biotronik and Medtronic have somewhat greater total activities of 3.082 Bq/Gy and 3.081 Bq/Gy, respectively. The activity of the St Jude model was almost three orders of magnitude smaller after activation by 10 MV X-rays than after 20 MV X-rays.

The dose rates from the gamma-rays emitted by the CIEDs activated

in the 20 MV beam were on the level of several hundred pGy/h immediately after the exposure to radiation. Of course, such dose rate does not pose a radiation risk to patients.

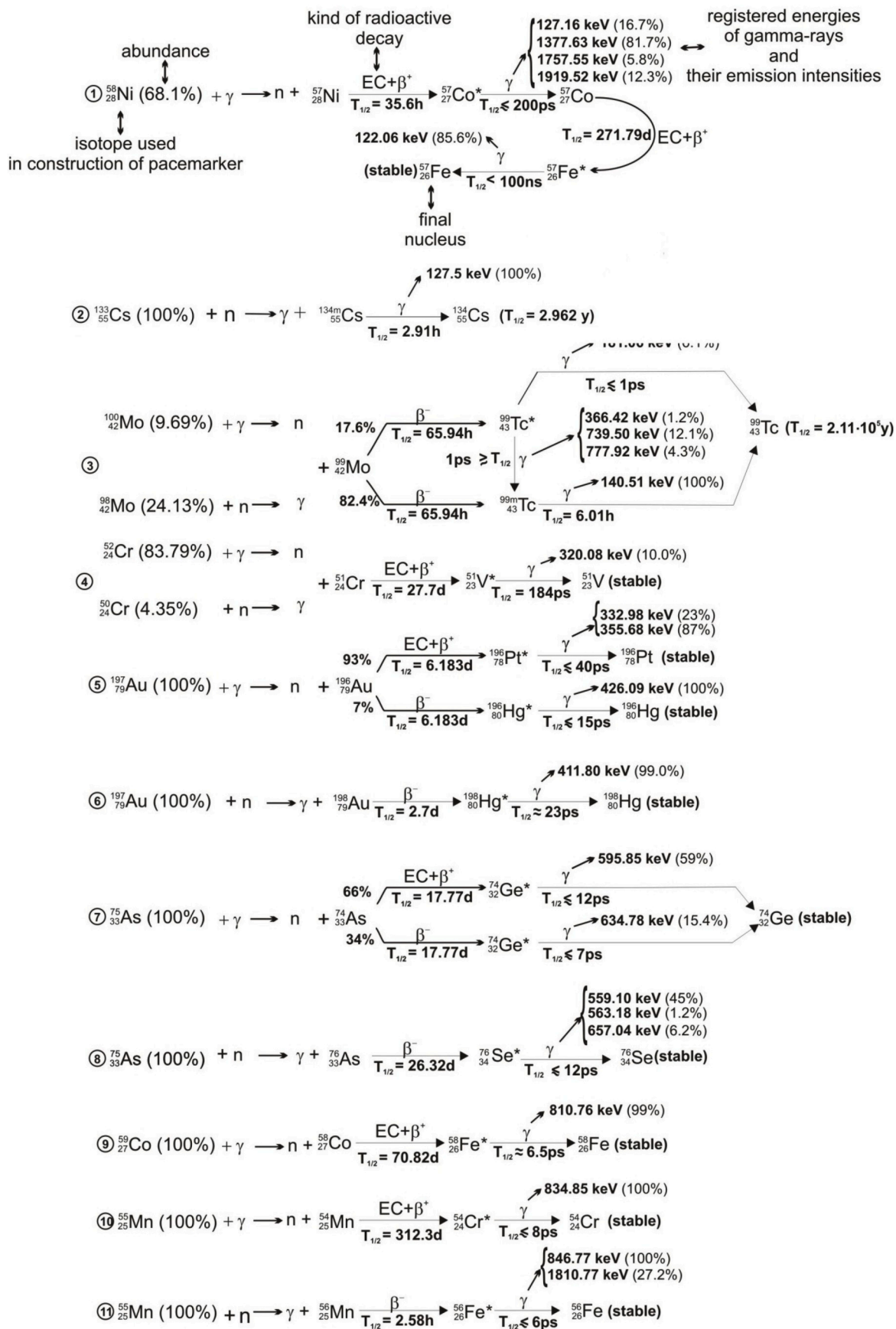


Fig. 9a. Identified nuclear reactions and radioactive decays (part 1).

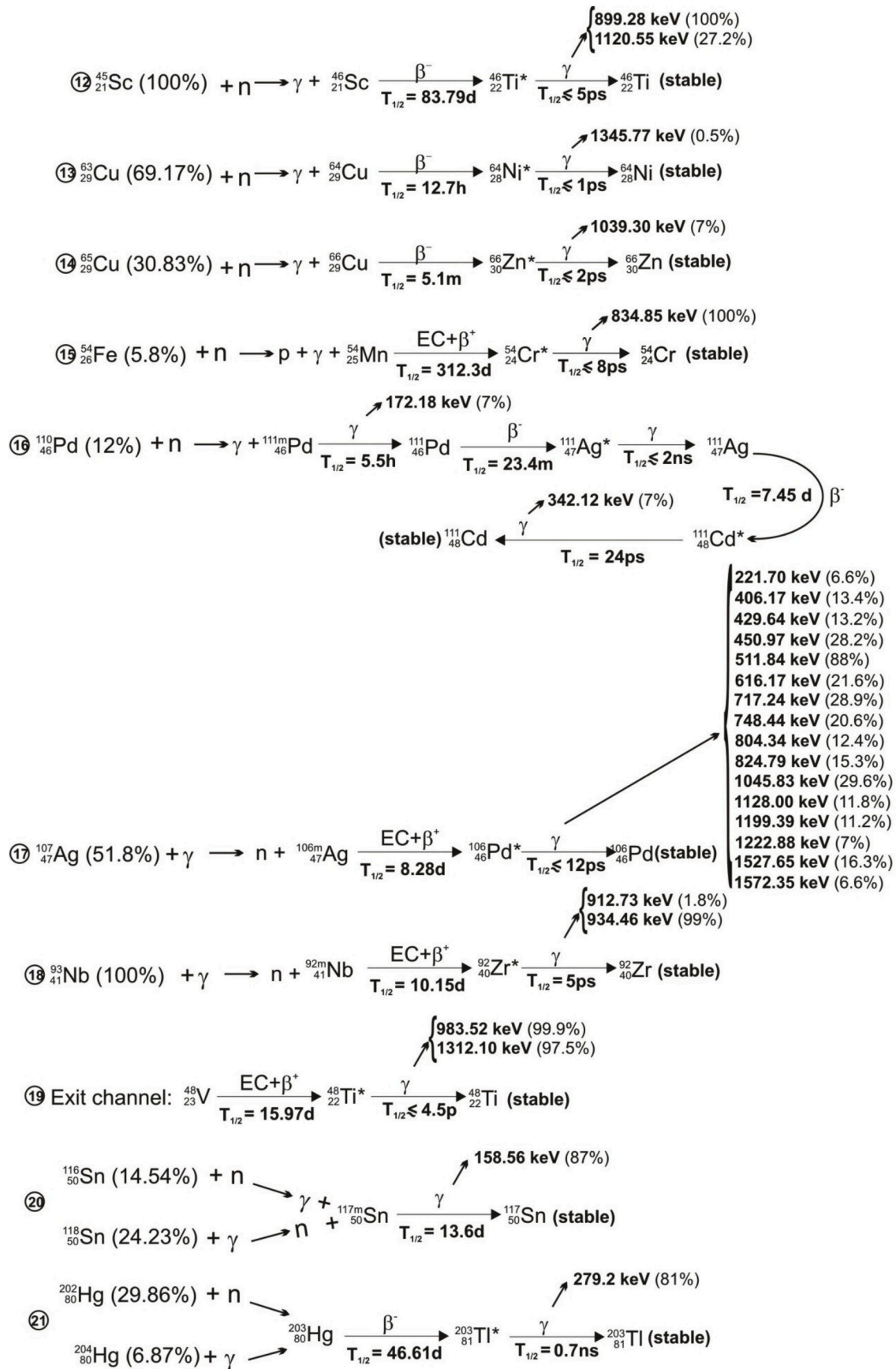


Fig. 9b. Identified nuclear reactions and radioactive decays (part 2).

Table 2

List of the identified radioisotopes and their activities for the considered models of CIEDs. The activities are related to the moment of the end of irradiation of CIEDs. The radioisotopes which can originate from the neutron reaction are denoted in bold.

St Jude 3213–36 Promote RF after irradiation of 20 MV X-rays		Biotronik Lumax 340 DR after irradiation of 20 MV X-rays		Medtronic Maximo II DR after irradiation of 20 MV X-rays		St Jude 3213–36 Promote RF after irradiation of 10 MV X-rays	
Activated isotope	Activity [Bq/Gy]	Activated isotope	Activity [Bq/Gy]	Activated isotope	Activity [Bq/Gy]	Activated isotope	Activity [Bq/Gy]
^{117m} Sn	1.048 ± 0.004	^{117m} Sn	1.147 ± 0.004	^{117m} Sn	1.840 ± 0.006	⁵⁴ Mn	0.004 ± <0.001
⁵⁷ Ni	0.374 ± 0.002	⁶⁶ Cu	0.830 ± 0.003	⁶⁶ Cu	0.542 ± 0.003	⁵⁷ Ni	0.002 ± <0.001
⁵¹ Cr	0.296 ± 0.002	⁵⁷ Ni	0.369 ± 0.002	⁶⁴ Cu	0.247 ± 0.002	⁵⁸ Co	0.002 ± <0.001
¹⁹⁶ Au	0.099 ± 0.001	⁵¹ Cr	0.366 ± 0.002	¹¹¹ Ag	0.094 ± 0.001	⁵⁶ Mn	0.002 ± <0.001
⁹⁹ Mo	0.072 ± 0.001	⁶⁴ Cu	0.140 ± 0.002	⁵⁷ Ni	0.089 ± 0.001	⁵⁷ Co	- **
⁵⁷ Co	0.056 ± <0.001	¹⁹⁶ Au	0.116 ± 0.002	¹⁹⁶ Au	0.069 ± <0.001		
^{99m} Tc	0.052 ± <0.001	⁵⁴ Mn	0.062 ± <0.001	⁴⁸ V	0.037 ± <0.001		
^{106m} Ag	0.040 ± <0.001	¹⁹⁸ Au	0.022 ± <0.001	^{92m} Nb	0.036 ± <0.001		
⁷⁴ As	0.036 ± <0.001	⁵⁷ Co	0.019 ± <0.001	⁷⁴ As	0.032 ± <0.001		
⁵⁶ Mn	0.032 ± <0.001	⁴⁶ Sc	0.011 ± <0.001	^{106m} Ag	0.028 ± <0.001		
⁷⁶ As	0.028 ± <0.001			⁴⁶ Sc	0.020 ± <0.001		
¹⁹⁸ Au	0.027 ± <0.001			⁵⁷ Co	0.018 ± <0.001		
⁵⁶ Ni	0.011 ± <0.001			⁷⁶ As	0.017 ± <0.001		
⁵⁸ Co	0.009 ± <0.001			¹⁹⁸ Au	0.014 ± <0.001		
⁵⁴ Mn	0.003 ± <0.001						

*The 122.06 keV photopeak is of much greater intensity than it results from the activity of ⁵⁷Ni. The cause of this was not identified and therefore the activity of ⁵⁷Co was not determined.

Table 3

Maximum cross sections for the identified photonuclear reactions and the corresponding energy (Dietrich and Bermab, 1998).

Photonuclear reaction	Maximum cross section
⁵² Cr(γ,n) ⁵¹ Cr	0.01 b at 20 MeV
⁵⁵ Mn(γ,n) ⁵⁴ Mn	0.07 b at 18 MeV
⁵⁸ Ni(γ,n) ⁵⁷ Ni	0.03 b at 17 MeV
⁵⁸ Ni(γ,2n) ⁵⁶ Ni	0.002 b at 25 MeV
⁵⁹ Co(γ,n) ⁵⁸ Co	0.08 b at 16 MeV
⁷⁵ As(γ,n) ⁷⁴ As	0.09 b at 16 MeV
⁹³ Nb(γ,n) ^{92m} Nb	0.2 b at 16 MeV
¹⁰⁰ Mo(γ,n) ⁹⁹ Mo	0.18 b at 15 MeV
¹⁰⁷ Ag(γ,n) ^{106m} Ag	0.2 b at 15 MeV
¹⁹⁷ Au(γ,n) ¹⁹⁶ Au	0.58 b at 14 MeV
¹¹⁸ Sn(γ,n) ^{117m} Sn	0.27 b at 15 MeV

Table 4

The simple capture cross sections σ_{ther} for thermal neutrons, the highest resonances in simple capture cross sections σ_{res} together with the corresponding energies for the neutron-induced reactions leading to the production of the identified radioisotopes with the highest activities. (<http://www.nndc.bnl.gov/s>).

Reaction	σ_{ther}^a	σ_{res}
¹¹⁶ Sn(n,γ) ^{117m} Sn	2.7 b	1651.6 b at 111.2 eV 121.9 b at 147.7 eV 87.4 b at 632.6 eV
⁵⁰ Cr(n,γ) ⁵¹ Cr	15.9 b	76 b at 5.462 keV
⁶³ Cu(n,γ) ⁶⁴ Cu	4.5 b	691.1 b at 578.9 eV
⁶⁵ Cu(n,γ) ⁶⁶ Cu	2.2 b	442.3 b at 230 eV
⁹⁸ Mo(n,γ) ⁹⁹ Mo	2.6 b	1310 b at 44.9 eV 546 b at 131.4 eV 375.1 b at 819 eV 335.6 b at 430 eV 217.1 b at 613 eV 161.6 b at 70.9 eV 79 b at 5.46 keV
¹¹⁰ Pd(n,γ) ^{111m} Pd	0.23 b	171.3 b at 263.3 eV 92.4 b at 899.9 eV 90.7 b at 1.004 keV

^a The values of σ_{ther} included in this table are related to the room temperature.

Table 5

β+/β-emitters induced in the CIEDs, decaying without emission of gamma-rays (Firestone, 1996).

Target isotope (abundance)	Nuclear reaction	Daughter radioisotope, T _{1/2}	Type and energy of decay
¹²⁰ Sn (32.59%)	¹²⁰ Sn (n,γ) ¹²¹ Sn	¹²¹ Sn, 27.06 h	β-, 388.1 keV
¹²² Sn (4.63%)	¹²² Sn(γ, n) ¹²¹ Sn		
¹²² Sn (4.63%)	¹²² Sn (n,γ) ¹²³ Sn	¹²³ Sn, 129.2 d	β-, 1404 keV
¹²⁴ Sn (5.79%)	¹²⁴ Sn(γ, n) ¹²³ Sn		
⁶³ Cu(69.17%)	⁶³ Cu(γ, n) ⁶² Cu	⁶² Cu, 9.74 m	EC + β+, 1404 keV

4. Discussion and conclusions

The identified nuclear reactions indicate that radiation damages and malfunctions may be expected in the CIEDs exposed to high-energy X-ray beams generated by medical linacs. The lower energy of the therapeutic beams, the lower activation of the CIEDs and the number of nuclear reactions in the CIEDs, particularly these induced by neutrons. Implant device manufacturers often label their products with warnings relating to the risk of radiation exposure of the devices. Previously mentioned, Recommendations and Protocol for the Management of the CIED Patient Undergoing Radiation Therapy (Indik et al., 2017) and the European Heart Rhythm Association survey (Lenarczyk et al., 2017) both stress that it is an evaluation of the CIEDs that is absolutely necessary before and during the radiation therapy and not their removal. However, the device may be temporarily explanted or irradiation may proceed with an appropriate gamma-ray shielding designed to reduce the device dose to less than approximately 10 Gy with the device operation continuously monitored (Bradley and Normand, 1998). Even then, though photons with energies greater than 8–10 MeV potentially generate neutrons through photonuclear reactions. In this work the consequences of the nuclear reactions occurring in the implanted cardiac devices were not studied. This problem is beyond the scope of our paper but additional effects from nuclear reactions cannot be excluded. The probability of reprogramming of the software code or bits is strongly connected with a transient charge disruption, thus, with the electric charge that can be induced by the particles with a high linear energy

transfer (LET) in the CIEDs. The gamma-ray radiation emitted in decay processes may induce the electric charge during ionization of atoms in photoelectric effect and in Compton scattering. The electric charge can also be induced by a direct ionization caused by electrons and positrons from the decays. As revealed in literature ionization caused by the decay products is insufficient to generate single event effects (Bradley and Normand, 1998). However, as it was noticed by Leray (2007), in the semiconductor part of a device, even the relatively small charges produced give rise to the overall current, by collection, diffusion, and any bipolar effects, such as amplification involving external supply. Moreover, the electric charge induced by gamma-rays, electrons and positrons can be accumulated in the insulating materials in the CIEDs. The effects of this charge accumulation are difficult to determine, they have not been investigated yet. It is worth noticing that ionization caused by the decay products can produce an electric charge in the CIEDs continuously, even several weeks after the last irradiation séance, because of the relatively long half-lives of several radioisotopes induced in such processes. Therefore, the cardio-oncologic patients with implanted cardiac devices should be monitored also after the radiotherapy completion. Systematic supervision of patients, especially those who have been subject to long-term radiation therapy, and evaluation of their CIEDs are necessary, because the probability of a CIED malfunction is expected to increase with time of exposition, due to accumulation of the radiation damages and of the electric charge induced by the ionization processes.

It is worth to notice that modern microelectronic devices and systems are now found to be sensitive to neutrons in the 1–10 MeV energy range as it was shown by Bisell et al. (Bisello et al., 2012). Thus not only neutrons produced directly in CIEDs, but also those originating from the collimator systems of medical accelerators are likely to induce SEEs.

The radioisotopes decaying with no gamma-ray emission are difficult to be identified. The β^+/β^- emitters can be partially deduced from the identified gamma-ray emitters. However, relatively short ranges of β^+/β^- radiation in solids cause that almost whole energy of electrons and positrons is absorbed directly by the CIEDs, thus excluding identification of radioisotopes decaying with no gamma-ray emission. Moreover, gamma emitters with half-lives of a minute or shorter could not be identified because they decayed before the beginning of the spectroscopic measurements.

It should be stressed that avoiding a direct exposure of the CIED to the radiation beam does not solve the problem of the nuclear reactions and the charge production in the irradiated device, because the neutron field is present in the whole treatment room. Simple neutron capture reactions are of special importance because they are usually characterized by large cross sections. Photonuclear reactions occurring only in the treatment beam are less important, because a cautious approach in treatment planning and during dose delivery give usually a possibility of some control over the CIEDs protection and the possible dose. A partial solution is to replace some materials with others. In particular, it should be recommended to eliminate the isotopes (^{116}Sn , ^{51}Cr , ^{64}Cu , ^{66}Cu , ^{55}Mn) with the high cross sections for simple capture reactions. We would also suggest considering the use of shields, absorbing decelerated neutrons, limited to the region around the CIEDs. Such a solution will be described in our next paper.

As the new generation CIEDs have not been verified yet in terms of the possible effects of their interaction with ionizing radiation, this study provides the first insight into the problem of the radiation safety of the construction materials of these devices. The present stage of our work is limited to the identification of the induced radioisotopes and the nuclear reactions occurring in the CIEDs. Such knowledge should be useful for the manufacturers of the medical electronic devices.

Declaration of competing interest

The authors declare that they have no known competing financial interests or personal relationships that could have appeared to influence

the work reported in this paper.

CRedit authorship contribution statement

Adam Konefal: Conceptualization, Methodology, Investigation, Resources, Writing - review & editing, Project administration, Data curation, Supervision, Formal analysis. **Slawomir Blamek:** Conceptualization, Methodology, Investigation, Resources, Writing - review & editing, Project administration. **Aleksandra Wronska:** Methodology, Investigation, Resources, Writing - review & editing. **Andrzej Orlef:** Investigation, Writing - review & editing. **Maria Sokół:** Investigation, Writing - review & editing. **Mateusz Tajstra:** Resources, Writing - review & editing. **Mariusz Gąsior:** Resources, Writing - review & editing.

References

- Alem-Bezoubiri, A., Bezoubiri, F., Badreddine, A., Mazrou, H., Lounis-Mokrani, Z., 2014. Monte Carlo estimation of photoneutrons spectra and dose equivalent around an 18 MV medical linear accelerator. *Radiat. Phys. Chem.* 97, 381–392.
- Barquero, R., Mendez, R., Iniguez, M.P., Vega-Carrillo, H.R., Voytchev, M., 2002. Thermoluminescence measurements of neutron dose around a medical LINAC. *Radiat. Protect. Dosim.* 101, 493–496.
- Baumann, R.C., 2001. Soft errors in advanced semiconductor devices-part I: the three radiation sources. *IEEE Trans. Device Mater. Reliab.* 1 (1), 17–22.
- Bieniasiewicz, M., Konefal, A., Wendykier, J., Orlef, A., 2016. Measurements of thermal and resonance neutron fluence and induced radioactivity inside bunkers of medical linear accelerators in the center of oncology in Opole, Poland. *Acta Phys. Pol. B* 47 (3), 771–776.
- Biltekin, F., Yeginer, M., Ozyigit, G., 2015. Investigating in-field and out-of-field neutron contamination in high-energy medical linear accelerators based on the treatment factors of field size, depth, beam modifiers, and beam type. *Phys. Med.* 31 (5), 517–523.
- Bisello, D., Candeloria, A., Dzysiuk, N., Esposito, J., Mastinu, P., Mattiazio, S., Prete, G., Silvestrina, L., Wyss, J., 2012. Neutron production targets for a new single event effects facility at the 70 MeV cyclotron of LNL-INFN. *Physics Procedia* 26, 284–293.
- Bitterman, D.S., Zei, P.C., Mak, R.H., 2018. Radiation safety and cardiovascular implantable electronic devices. *Int J Radiat Oncol* 102 (2), 243–246.
- Blamek, S., Gabryś, D., Kulik, R., Kruczek, A., Miszczyk, L., 2014. Stereotactic body radiosurgery, robotic radiosurgery and tomotherapy in patients with pacemakers and implantable cardioverters-defibrillators: mini-review. *Exp. Clin. Cardiol.* 20 (7), 757–763.
- Blamek, S., Tajstra, M., Gadula-Gacek, E., Gabryś, D., Niewiadomska, B., Bekman, A., Dolla, L., Gąsior, M., 2016. Effect of radiation therapy delivered with helical tomotherapy technique on latest generation of implantable cardioverters-defibrillators (ICD) and cardiac resynchronization therapy-defibrillator (CRT-D) devices. *Int. J. Radiat. Oncol. Biol. Phys.* 96 (2), E611.
- Bradley, P.D., Normand, E., 1998. Single event upsets in implantable cardioverter defibrillators. *IEEE Trans. Nucl. Sci.* 45 (6), 2929–2940.
- Brambatti, M., Mathew, R., Strang, B., et al., 2015. Management of patients with implantable cardioverter-defibrillators and pacemakers who require radiation therapy. *Heart Rhythm* 12 (10), 2148–2154.
- Choi, Chang Heon, Park, So-Yeon, Park, Jong Min, Chun, Minsoo, Kim, Jung-in, 2018. Monte Carlo simulation of neutron dose equivalent by photoneutron production inside the primary barriers of a radiotherapy vault. *Phys. Med.* 48, 1–5.
- Dietrich, S.S., Bermab, B.L., 1998. Atlas of photoneutron cross sections obtained with monoenergetic photons. *Atomic Data Nucl. Data Tables* 38, 199–338.
- Ditrói, F., Tárkányi, F., Takács, S., Hermanne, A., 2016. Activation cross sections of proton induced nuclear reactions on gold up to 65 MeV. *Appl. Radiat. Isot.* 113, 96–109.
- Dong, A.X., Gwinn, R.P., Warner, N.M., Caylor, L.M., Doherty, M.J., 2016. Mitigating bit flips or single event upsets in epilepsy neurostimulators. *Epilepsy & Behavior Case Reports* 5, 72–74.
- Elham, Hosseinzadeh, Nooshin, Banaee, Ali, Nedaie Hassan, 2018. Monte Carlo calculation of photo-neutron dose produced by circular cones at 18 MV photon beams. *Rep. Practical Oncol. Radiother.* 23 (1), 39–46.
- Esposito, A., Bedogni, R., Lembo, L., Morelli, M., 2008. Determination of the neutron spectra around an 18 MV medical linac with a passive Bonner sphere spectrometer based on gold foils and TLD pairs. *Radiat. Meas.* 43, 1038–1043.
- Firestone, R.B. (Ed.), 1996. *Table of Isotopes*, eighth ed. University of California: Lawrence Berkeley National Laboratory. version 1.0.
- Gauter-Fleckenstein, B., Israel, C.W., Dorenkamp, M., Dunst, J., Roser, M., Schimpf, R., Steil, V., Schäfer, J., Höller, U., Wenz, F., 2015. DEGRO/DGK guideline for radiotherapy in patients with cardiac implantable electronic devices. *Strahlenther. Onkol.* 191, 393–404.
- Hashemi, S.M., Hashemi-Malayeri, B., Raisali, G., Shokrani, P., Sharafi, A.A., 2007. A study of the photoneutron dose equivalent resulting from a Saturne 20 medical linac using Monte Carlo method. *Nukleonika* 52, 39–43.
- Howell, R.M., Kry, S.F., Burgett, E., Hertel, N.E., Followill, D.S., 2009. Secondary neutron spectra from modern Varian, Siemens and Elekta linacs with multileaf collimators. *Med. Phys.* 36, 4027–4038.
- <http://www.nndc.bnl.gov/sigma/search.jsp>.

- Hurkmans, C.W., Kneijens, J.L., Oei, B.S., Maas, A.J., Uiterwaal, G.J., van der Borden, A. J., Ploegmakers, M.M., van Erven, L., 2012. Management of radiation oncology patients with a pacemaker or ICD: a new comprehensive practical guideline in The Netherlands. Dutch Society of Radiotherapy and Oncology (NVRO). *Radiat. Oncol.* 24 (7), 198.
- Indik, J.H., Gimbel, J.R., Abe, H., et al., 2017. HRS expert consensus statement on magnetic resonance imaging and radiation exposure in patients with cardiovascular implantable electronic devices. *Heart Rhythm* 14 (7), e97–e153, 2017.
- Janiszewska, M., Polaczek-Grelak, K., Raczkowski, M., Szafron, B., Konefal, A., Zipper, W., 2014. Secondary radiation dose during high-energy total body irradiation. *Strahlenther. Onkol.* 190 (5), 459–466.
- Keehan, S., Taylor, M.L., Smith, R.L., Dunn, L., Kron, T., Franich, R.D., 2016. Dose and gamma-ray spectra from neutron-induced radioactivity in medical linear accelerators following high-energy total body irradiation. *Radiat. Protect. Dosim.* 172 (4), 327–332.
- Konefal, A., Dybek, M., Zipper, W., Łobodziec, W., Szczucka, K., 2005. Thermal and epithermal neutrons in the vicinity of the Primus Siemens biomedical accelerator. *Nukleonika* 50 (2), 73–81.
- Konefal, A., Orlef, A., Dybek, M., Maniakowski, Z., Polaczek-Grelak, K., Zipper, W., 2008a. Correlation between radioactivity induced inside the treatment room and the undesirable thermal/resonance neutron radiation produced by linac. *Phys. Med.* 24, 212–218.
- Konefal, A., Polaczek-Grelak, K., Zipper, W., 2008b. Undesirable nuclear reactions and induced radioactivity as a result of the use of the high-energy therapeutic beams generated by medical linacs. *Radiat. Protect. Dosim.* 128 (2), 133–145.
- Konefal, A., Orlef, A., Bieniasiewicz, M., 2016. Measurements of neutron radiation and induced radioactivity for the new medical linear accelerator, the Varian TrueBeam. *Radiat. Meas.* 86, 8–15, 2016.
- Kry, S.F., Salehpour, M., Followill, D.S., Stovall, M., Kuban, D.A., White, R.A., Rosen, L.I., 2005. Out-of-Field photon and neutron dose equivalents from step-and-shoot intensity-modulated radiation therapy. *Int. J. Radiat. Oncol. Biol. Phys.* 62 (4), 1204–1216.
- Lenarczyk, R., Potpara, T.S., Haugaa, K.H., Deharo, J.C., Hernandez-Madrid, A., Pineda, M.C.E., Kiliszek, M., Dągry, N., 2017. Approach to cardio-oncologic patients with special focus on patients with cardiac implantable electronic devices planned for radiotherapy: results of the European Heart Rhythm Association survey. *EP Europace* 19 (9), 1579–1584.
- Leray, J.L., 2007. Effects of atmospheric neutrons on devices, at sea level and in avionics embedded systems. *Microelectron. Reliab.* 47, 1827–1835.
- Ma, A., Awotwi-Pratt, J., Alghamdi, A., Alfuraih, A., Spyrou, N.M., 2002. Monte Carlo study of photoneutron production in the Varian Clinac 2100C linac. *J. Radioanal. Nucl. Chem.* 276, 119–123.
- Mao, X.S., Kase, K.R., Liu, J.C., Nelson, W.R., Kleck, J.H., Johnsen, S., 1997. Neutron sources in the Varian Clinac 2100C/2300C medical accelerator calculated by the EGS4 code. *Health Phys.* 72, 524–529.
- Mollerus, M., Naslund, L., Lipinski, M., Meyer, A., Libey, B., Dornfeld, K., 2014. Radiation tolerance of contemporary implantable cardioverter-defibrillators. *J. Intervent. Card Electrophysiol.* 39 (2), 171–175.
- O’Gorman, T.J., Ross, J.M., Taber, A.H., Ziegler, J.F., Muhlfeld, H.P., Montrose, I.C.J., et al., 1996. Field testing for cosmic ray soft errors in semiconductor memories. *IBM J. Res. Dev.* 40 (1), 41–50, 1996.
- Polaczek-Grelak, K., Karaczyn, B., Konefal, A., 2012. Nuclear reactions in linear medical accelerators and their exposure consequences. *Appl. Radiat. Isot.* 70, 2332–2339.
- Santa, S.A., 2017. Experimental validation of ex-vessel neutron spectrum by means of dosimeter materials activation method. *At. Indones.* 43 (1), 7–18.
- * Talebi, Asra Sadat, Hejazi, Payman, Jadidi, Majid, Ghorbani, Raheb, 2016. A Monte Carlo study on Photoneutron Spectrum around Elekta SL75/25 18 MV linear accelerator. *International Journal of Advanced Biological and Biomedical Research* 4 (1), 48–57.
- Vega Carrillo, H.R., Baltazar-Raigosa, A., 2011. Photoneutron spectra around an 18 MV linac. *J. Radioanal. Nucl. Chem.* 287, 323–327.
- Vega-Carrillo, H.R., Martinez-Ovalle, S.A., Lallena, A.M., Mercado, G.A., Benites-Rengifo, J.L., 2012. Neutron and photon spectra in LINACs. *Appl. Radiat. Isot.* 71, 75–80. Supplement: S.
- Vega-Carrillo, H.R., Leon-Martinez, H.A., Rivera-Perez, E., Benites-Rengifo, J.L., Gallego, E., Lorente, A., 2015. Induced radioisotopes in a linac treatment hall. *Appl. Radiat. Isot.* 102, 103–108.
- Wang, Q.B., Masumoto, K., Bessho, K., Matsumura, H., Miura, T., Shibata, T., 2007. Evaluation of the radioactivity in concrete from accelerator facilities. *J. Radioanal. Nucl. Chem.* 273, 55–58.
- Zaremba, T., Jakobsen, A.R., Søgaard, M., et al., 2015. Risk of device malfunction in cancer patients with implantable cardiac device undergoing radiotherapy: a population-based cohort study. *PACE - Pacing Clin Electrophysiol.* 38 (3), 343–356.
- Zecchin, M., Severgnini, M., Fiorentino, A., et al., 2018. Management of patients with cardiac implantable electronic devices (CIED) undergoing radiotherapy. *Int. J. Cardiol.* 255, 175–183.